Electronic Supplementary Material (ESI) for ChemComm.
This journal is © The Royal Society of Chemistry 2015

A dual-responsive supra-amphiphile based on a water soluble pillar[7]arene and a naphthalene diimide-containing guest†

Li Shao, Jiong Zhou, Bin Hua and Guocan Yu*

Department of Chemistry, Zhejiang University, Hangzhou 310027, P. R. China;

Email address: guocanyu@zju.edu.cn

Electronic Supplementary Information (21 pages)

1. *Materials and methods* S2
2. *Syntheses of* ***G₀*** *and* ***G*** S3
3. *Syntheses of* ***M₀*** *and* ***M*** S8
4. *2D COSY spectrum of* ***M*** *in* D_2O S12
5. *The sizes of pillar[5]arenes, pillar[6]arenes, pillar[7]arenes and* ***M*** S12
6. ^{1}*H NMR spectroscopy investigations of* ***WP7⊃M***, ***WP6⊃M*** *and* ***WP5⊃M*** S14
7. *Critical aggregation concentration (CAC) determinations of* ***G*** *and* ***WP7⊃G*** S15
8. *Dynamic light scattering (DLS) results of* ***WP7⊃G*** *in the absence and presence of 1 equiv. α-CD* S16
9. *The* ^{1}*H NMR of* ***WP7⊃M*** *with different molar ratios* S17
10. *Enlarged TEM images of* ***WP7⊃G*** *in the presence of 1 equiv. α-*CD S17
11. *ITC investigations of host−guest complexation between* ***WP7*** *and* ***M***, ***WP6*** *and* ***M***, ***WP5*** *and* ***M***, ***M*** *and α-CD,* ***WP7⊃M*** *and α-CD* S18
12. *Fluorescence spectroscopy studies of* ***M*** *and* ***WP7⊃M*** *after the addition of α-*CD S20
13. *2D NOESY NMR spectrum of* ***M*** *and α-CD in* D_2O S21

1. Materials and methods

All reagents were commercially available and used as supplied without further purification. Water-soluble pillar[7]arene **WP7** was synthesized according to literature procedures.[S1] Solvents were either employed as purchased or dried according to procedures described in the literature. ^{1}H NMR and ^{13}C NMR spectra were recorded on a Bruker Avance DMX 400 spectrophotometer or a Bruker Avance DMX 500 spectrophotomete. The 2D NOESY NMR spectrum was recorded on a Bruker Avance DMX 600 spectrophotometer with TMS as the internal reference. Low-resolution electrospray ionization mass spectra (LRESI-MS) were obtained on a Bruker Esquire 3000 Plus spectrometer (Bruker-Franzen Analytik GmbH Bremen, Germany) equipped with an ESI interface and an ion trap analyzer. High-resolution electrospray ionization mass spectra (HRESI-MS) were obtained on a Bruker 7-Tesla FT-ICR mass spectrometer equipped with an electrospray source (Billerica, MA, USA). The melting points were collected on a SHPSIC WRS-2 automatic melting point apparatus. UV-vis spectroscopy was performed on a Shimadzu UV-2550 instrument at room temperature. The fluorescence experiments were conducted on a RF-5301 spectrofluorophotometer (Shimadzu Corporation, Japan). Dynamic light scattering measurements were performed on a Nano-ZS ZEN3600 instrument.

2. Syntheses of ***G₀*** *and* ***G***

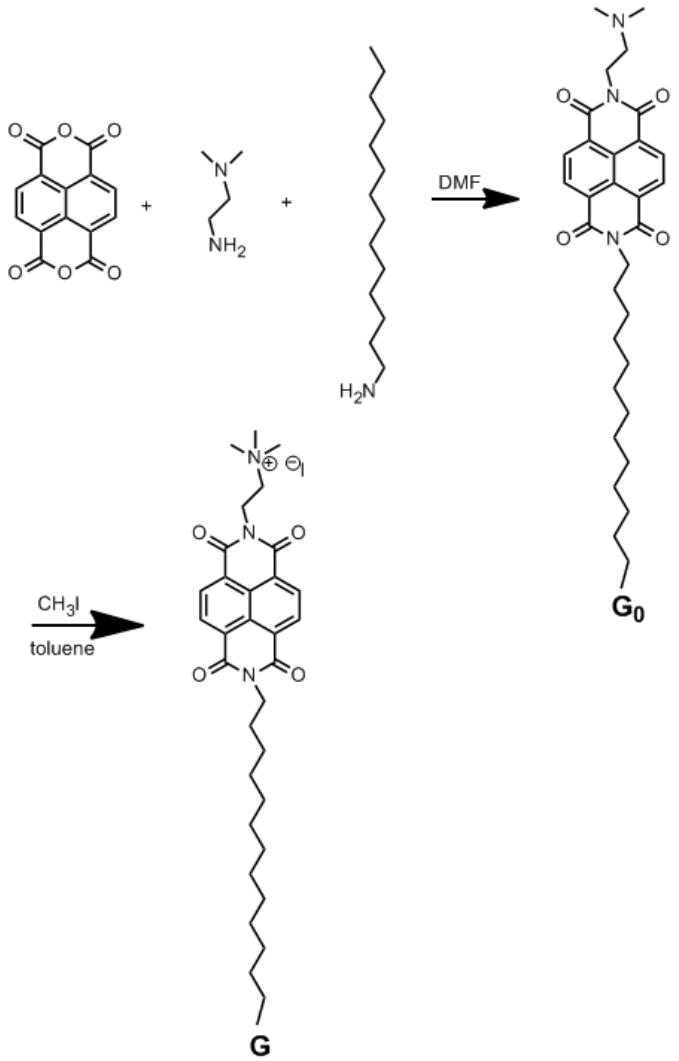

Scheme S1. Synthetic route to **G**.

Synthesis of $\mathbf{G_0}$: 1,4,5,8-Naphthalenetetracarboxylic dianhydride (4.02 g, 15.0 mmol), *N*,*N′*-dimethylaminoethylamine (1.32 g, 15.0 mmol), and 1-aminotetradecane (3.20 g, 15.0 mmol) were added into DMF. The mixture was heated in a flask under nitrogen atmosphere at 90 °C for 24 h. The solvent was removed by rotary evaporation and the crude product was isolated by column chromatography (silica gel; petroleum ether:CH_2Cl_2 = 10:1) to afford a dark red solid $\mathbf{G_0}$ (3.05 g, 38%). M.p. 148.3−150.2 °C. The proton NMR spectrum of $\mathbf{G_0}$ is shown in Fig. S1. ^{1}H NMR (400 MHz, $CDCl_3$, room temperature) δ (ppm): 8.75 (s, 4H), 4.35 (t, J = 8 Hz, 2H), 4.19 (t, J = 8 Hz, 3H), 2.68 (t, J = 4 Hz, 2H), 2.34 (s, 6H), 1.76−1.72 (m, 4H), 1.38−1.25 (m, 20H), 0.88 (t, J = 8 Hz, 3H). The ^{13}C NMR spectrum of $\mathbf{G_0}$ is shown in Fig. S2. ^{13}C NMR (100 MHz,

$CDCl_3$, room temperature) δ(ppm): 162.95, 162.75, 131.01, 130.92, 126.76, 126.68, 126.58, 56.94, 45.61, 41.01, 38.65, 31.92, 29.77, 29.69, 29.66, 29.66, 29.64, 29.60, 29.53, 29.36, 29.33, 28.08, 27.09, 22.69, 14.13. LRESIMS is shown in Fig. S3: *m*/*z* 534.6 $[M + H]^+$ (100%). HRESIMS: *m*/*z* calcd for $[M + H]^+$ $C_{32}H_{44}N_3O_4^+$, 534.3332; found 534.3335; error 0.6 ppm.

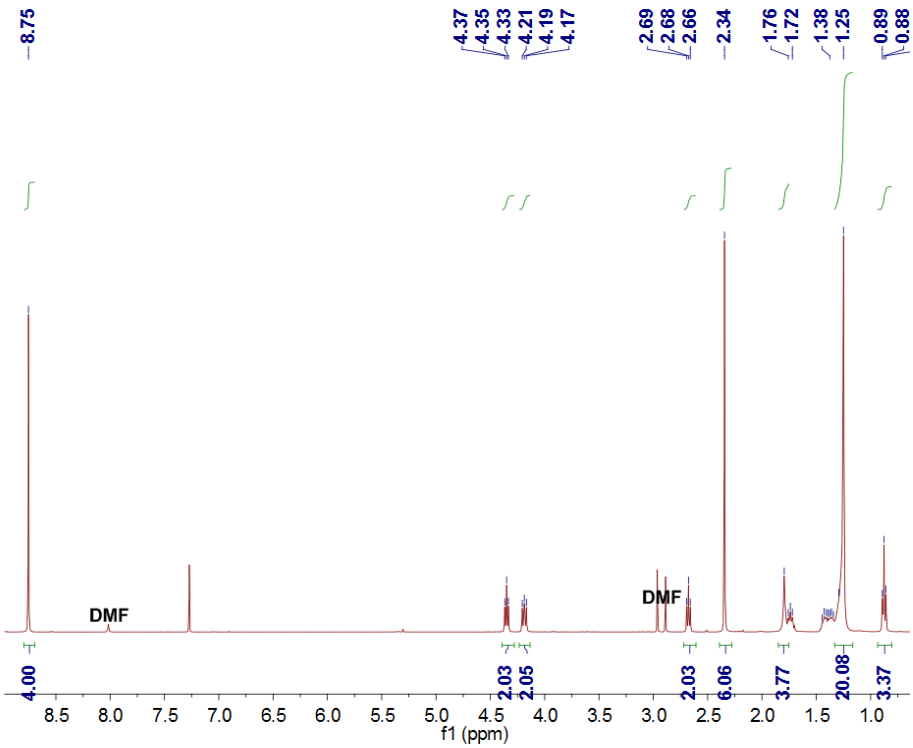

Fig. S1 ^{1}H NMR spectrum (400 MHz, $CDCl_3$, room temperature) of $\mathbf{G_0}$.

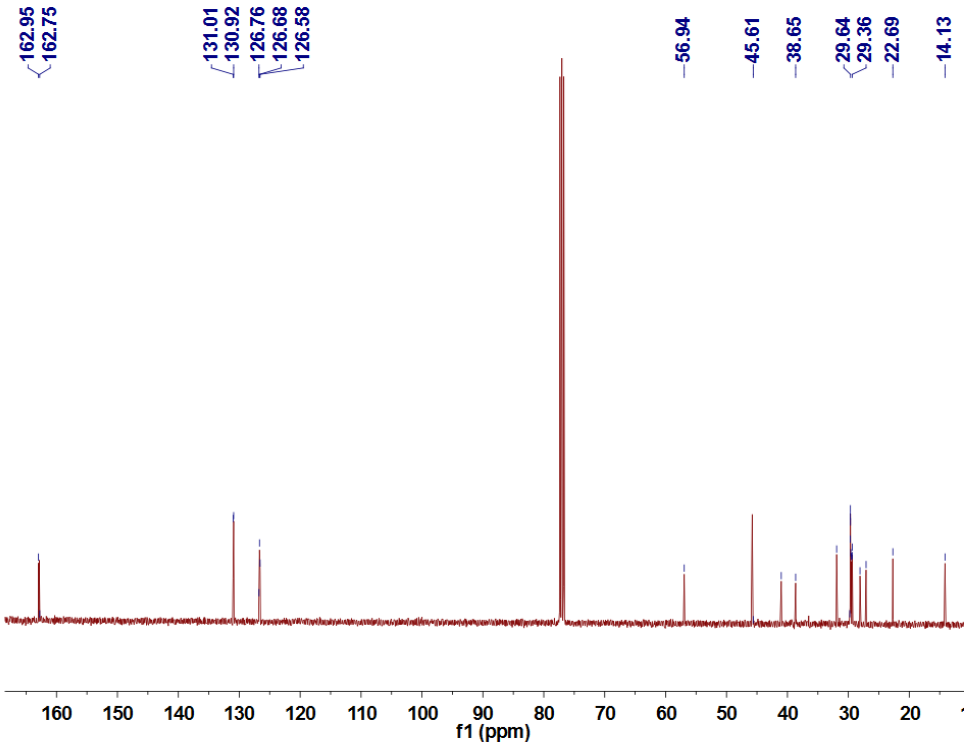

Fig. S2 ^{13}C NMR spectrum (100 MHz, $CDCl_3$, room temperature) of $\mathbf{G_0}$.

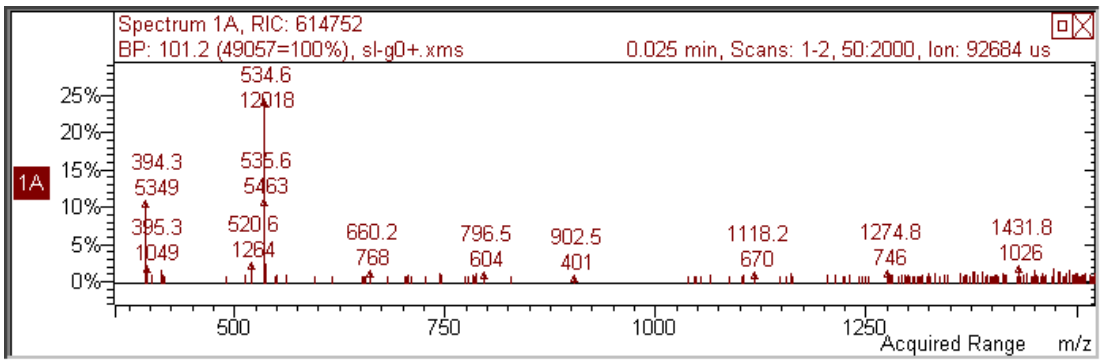

Fig. S3 Electrospray ionization mass spectrum of $\mathbf{G_0}$. Assignment of main peaks: *m/z* 534.6 $[M + H]^+$.

Synthesis of **G**: Excess CH_3I (5.00 g, 35.2 mmol) was added into a toluene solution of $\mathbf{G_0}$ (6.00 g, 11.2 mmol). The mixture was stirred at 40 °C for 24 h. Then the product was filtered and dried under vacuum to afford a light yellow solid **G** (5.75 g, 76%). M.p. 216.2−217.5 °C. The proton NMR spectrum of **G** is shown in Fig. S4. ^{1}H NMR (400 MHz, DMSO-d_6, room temperature) δ (ppm): 7.26 (t, J = 8.0 Hz, 2H), 7.17−7.12 (m, 2H), 3.65 (s, 2H), 3.26 (s, 9H), 2.29 (s, 2H), 1.65 (s, 2H), 1.33 (s, 2H), 1.24−1.22 (m, 24H), 0.84 (t, J = 8.0 Hz, 3H). The ^{13}C NMR spectrum of **G** is shown in Fig. S5. ^{13}C NMR (100 MHz, DMSO-d_6, room temperature) δ(ppm): 137.29, 128.85, 128.15, 125.27, 52.46, 31.27, 29.16, 29.02, 28.99, 28.95, 28.86, 28.80, 28.76, 28.69, 28.61, 28.58, 26.47, 22.07, 21.01, 13.92. LRESIMS is shown in Fig. S6: m/z 548.4 $[M - I]^+$ (100%). HRESIMS: m/z calcd for $[M - I]^+$ $C_{33}H_{46}N_3O_4^+$, 548.3488; found 548.3478; error −1.8 ppm.

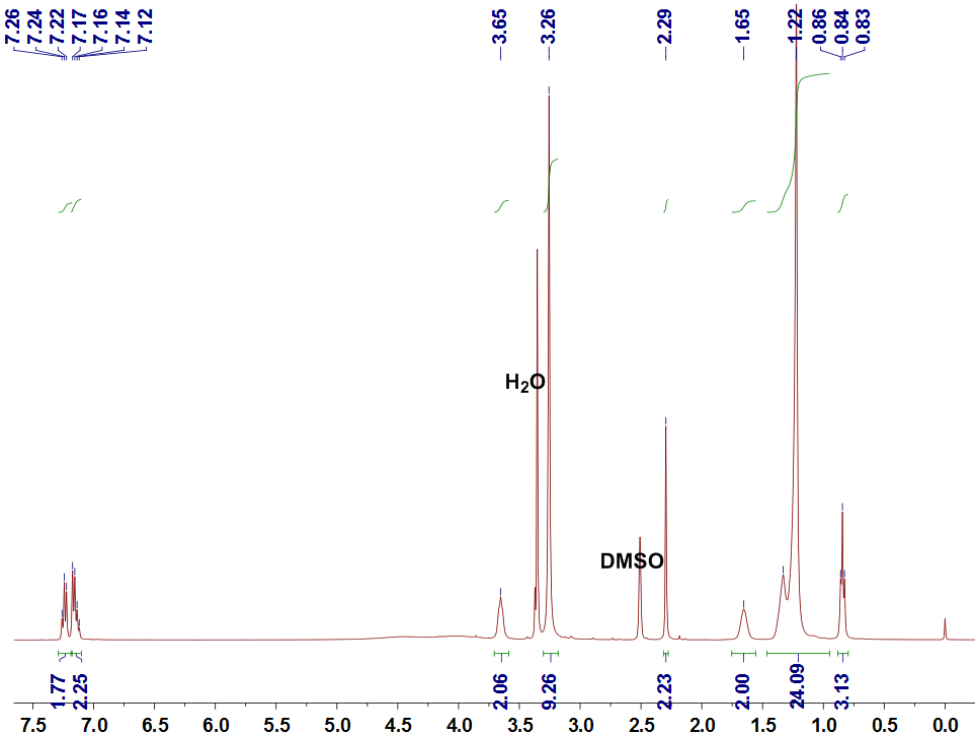

Fig. S4 ^{1}H NMR spectrum (400 MHz, DMSO-d_6, room temperature) of **G**.

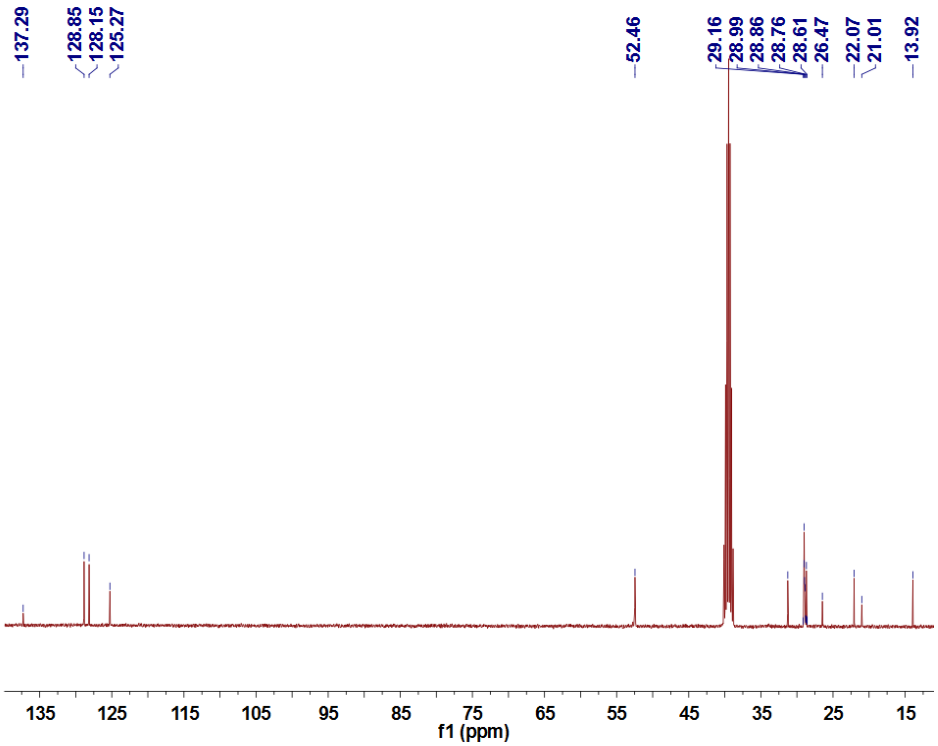

Fig. S5 ^{13}C NMR spectrum (100 MHz, DMSO-d_6, room temperature) of **G**.

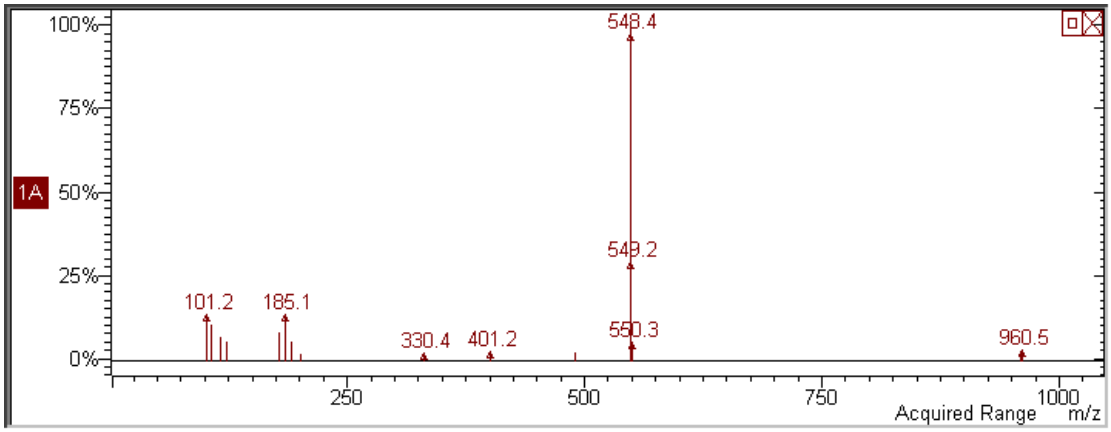

Fig. S6 Electrospray ionization mass spectrum of **G**. Assignment of main peaks: *m*/*z* 548.4 $[M - I]^+$.

3. Syntheses of ***M₀*** *and* ***M***

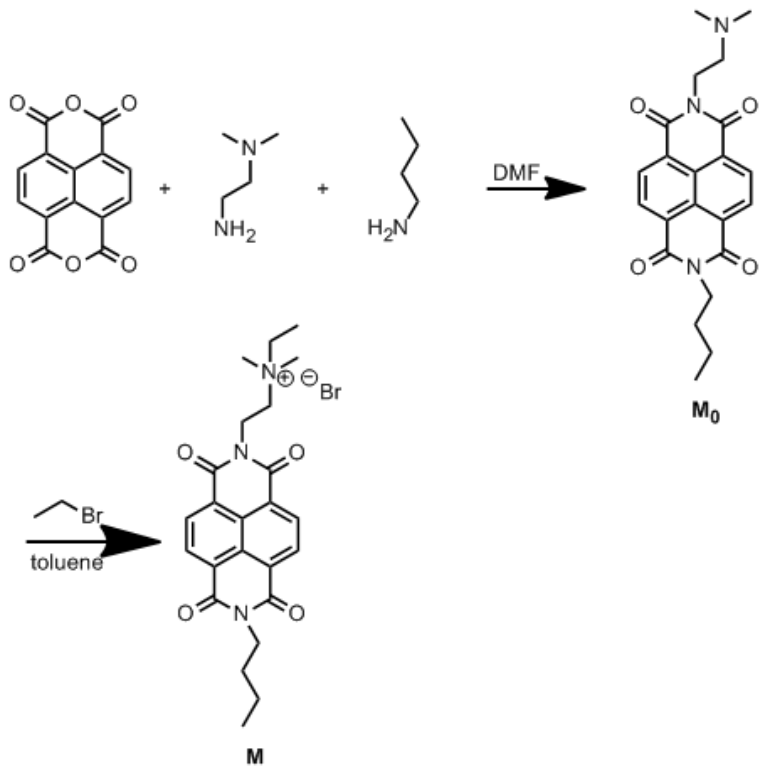

Scheme S2. Synthetic route to **M**.

Synthesis of $\mathbf{M_0}$: 1,4,5,8-Naphthalenetetracarboxylic dianhydride (3.40 g, 12.7 mmol), *N*,*N′*-dimethylaminoethylamine (1.10 g, 12.7 mmol), and butylamine (0.950 g, 12.7 mmol) were dissolved in DMF. The mixture was heated in a flask under nitrogen atmosphere at 90 °C for 24 h. The solvent was removed by rotary evaporation and the crude product was isolated by column chromatography (silica gel; petroleum ether:CH_2Cl_2 = 10:1) to get a dark red solid $\mathbf{M_0}$ (1.5 g, 30%). M.p. 179.4−180.5 °C. The proton NMR spectrum of $\mathbf{M_0}$ is shown in Fig. S7. ^{1}H NMR (400 MHz, $CDCl_3$, room temperature) δ (ppm): 8.76 (s, 4H), 4.35 (t, J = 8.0 Hz, 2H), 4.21 (t, J = 8.0 Hz, 2H), 2.67 (t, J = 8.0 Hz, 4H), 1.73−1.70 (m, 2H), 1.45−1.42 (m, 2H), 0.99 (t, J = 8.0 Hz, 3H). The ^{13}C NMR spectrum of $\mathbf{M_0}$ is shown in Fig. S8. ^{13}C NMR (125 MHz, $CDCl_3$, room temperature) δ (ppm): 162.91, 162.81, 162.55, 130.98, 130.89, 126.72, 126.64, 126.56, 56.93, 45.77, 40.74, 38.63, 30.14, 20.33, 13.81. LRESIMS is shown in Fig. S9: *m*/*z* 394.4 $[M + H]^+$ (100%). HRESIMS: *m*/*z* calcd for $[M + H]^+$ $C_{22}H_{24}N_3O_4^+$, 394.1767; found 394.1762; error −1 ppm.

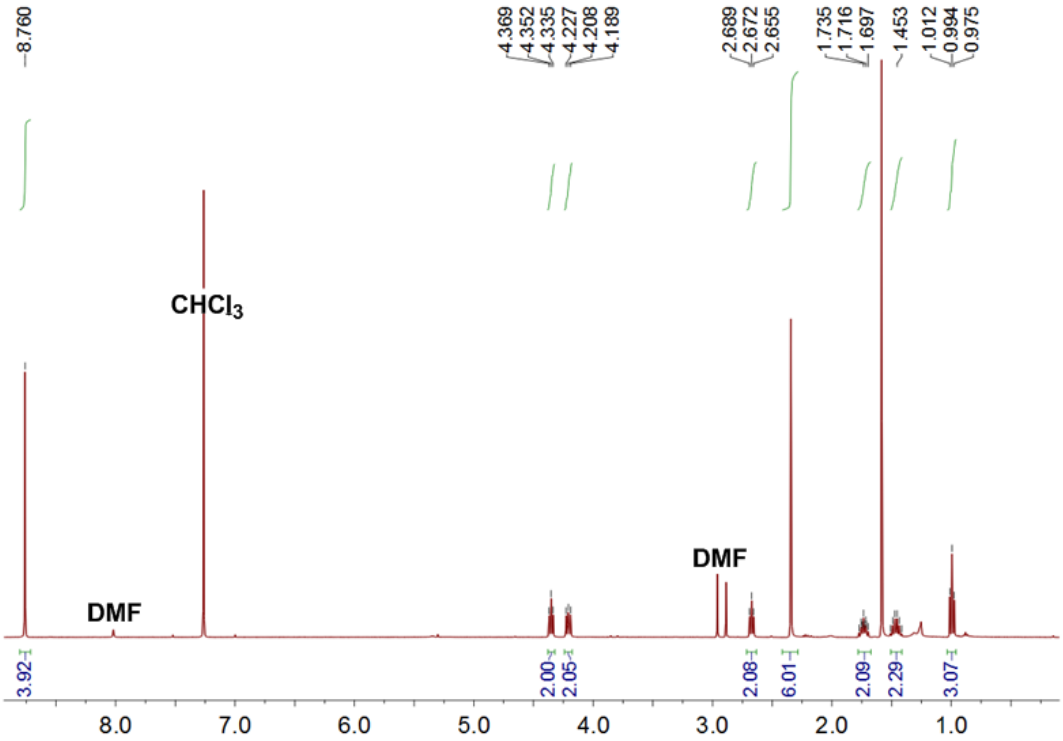

Fig. S7 ^{1}H NMR spectrum (400 MHz, $CDCl_3$, room temperature) of $\mathbf{M_0}$.

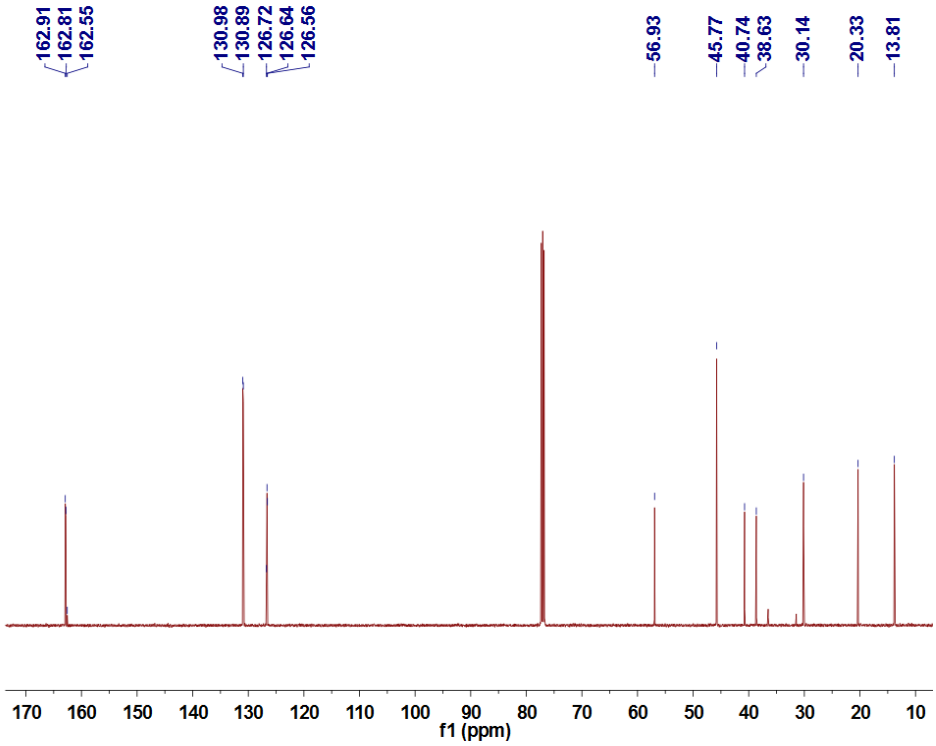

Fig. S8 ^{13}C NMR spectrum (125 MHz, $CDCl_3$, room temperature) of $\mathbf{M_0}$.

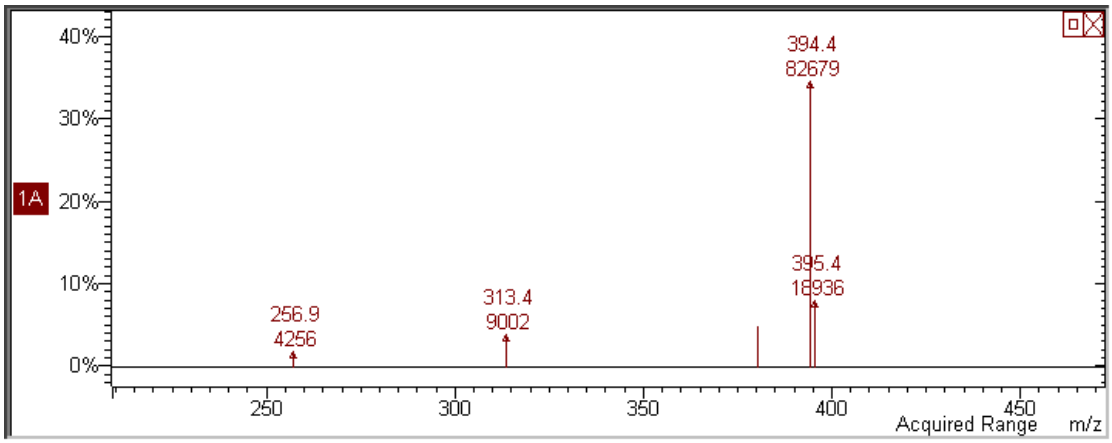

Fig. S9 Electrospray ionization mass spectrum of $\mathbf{M_0}$. Assignment of main peak: *m*/*z* 394.4 $[M + H]^+$.

Synthesis of **M**: Excess bromoethane (2.60 g, 23.9 mmol) was added into a toluene solution of $\mathbf{M_0}$ (4.00 g, 7.96 mmol). The mixture was heated in a flask under nitrogen atmosphere at reflux for 24 h. The product was filtered and dried under vacuum to get a red solid **M** (5.57 g, 87%) M.p. 261.4−262.1 °C. The proton NMR spectrum of **M** is shown in Fig. S10. ^{1}H NMR (400 MHz, D_2O, room temperature) δ (ppm): 8.47−8.37 (m, 4H), 4.52 (t, J = 8.0 Hz, 2H), 3.92 (d, J = 8.0 Hz, 2H), 3.50 (m, 4H), 3.19 (s, 6H), 1.56 (m, 2H), 1.40 (t, J = 8.0 Hz, 3H), 1.32 (m, 2H), 0.88 (t, J = 8.0 Hz, 3H). The ^{13}C NMR spectrum of **M** is shown in Fig. S11. ^{13}C NMR (100 MHz, DMSO-d_6, room temperature) *ä* (ppm): 162.69, 162.55, 130.50, 130.41, 126.56, 126.24, 126.16, 126.13, 58.95, 58.23, 49.75, 33.16, 29.52, 19.82, 13.66, 7.79. LRESIMS is shown in Fig. S12: *m*/*z* 422.2 $[M - Br]^+$ (100%). HRESIMS: *m*/*z* calcd for $[M - Br]^+$ $C_{24}H_{28}N_3O_4^+$, 422.2080; found 422.2063; error −4.0 ppm.

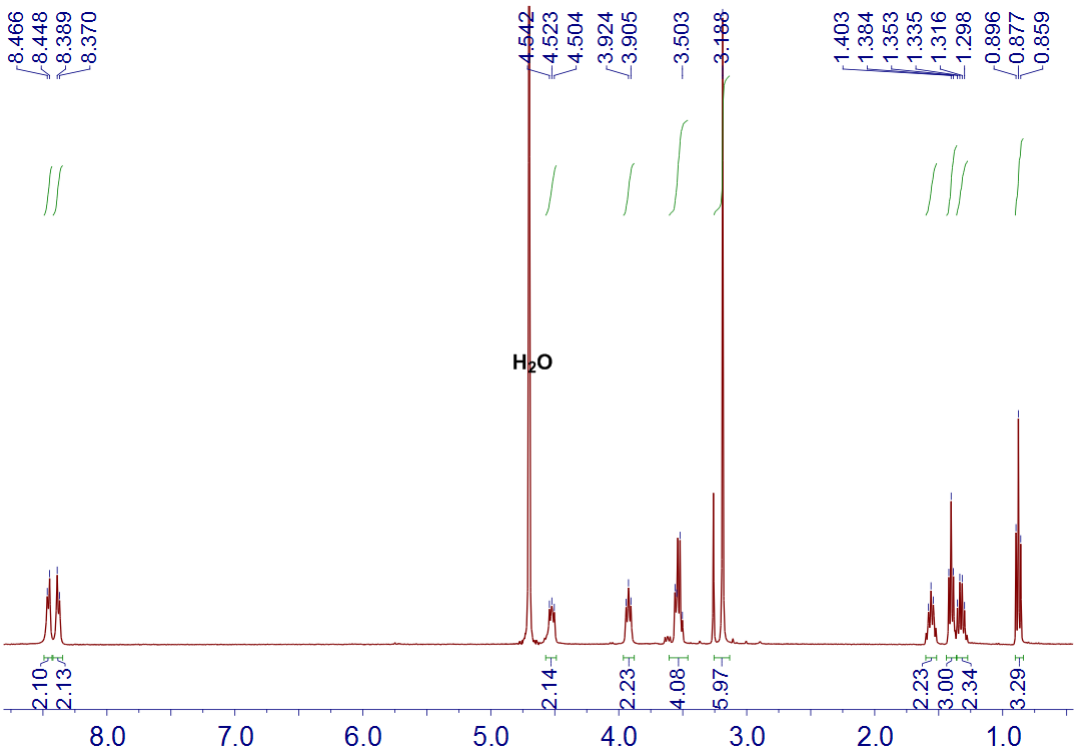

Fig. S10 ^{1}H NMR spectrum (400 MHz, D_2O, room temperature) of **M**.

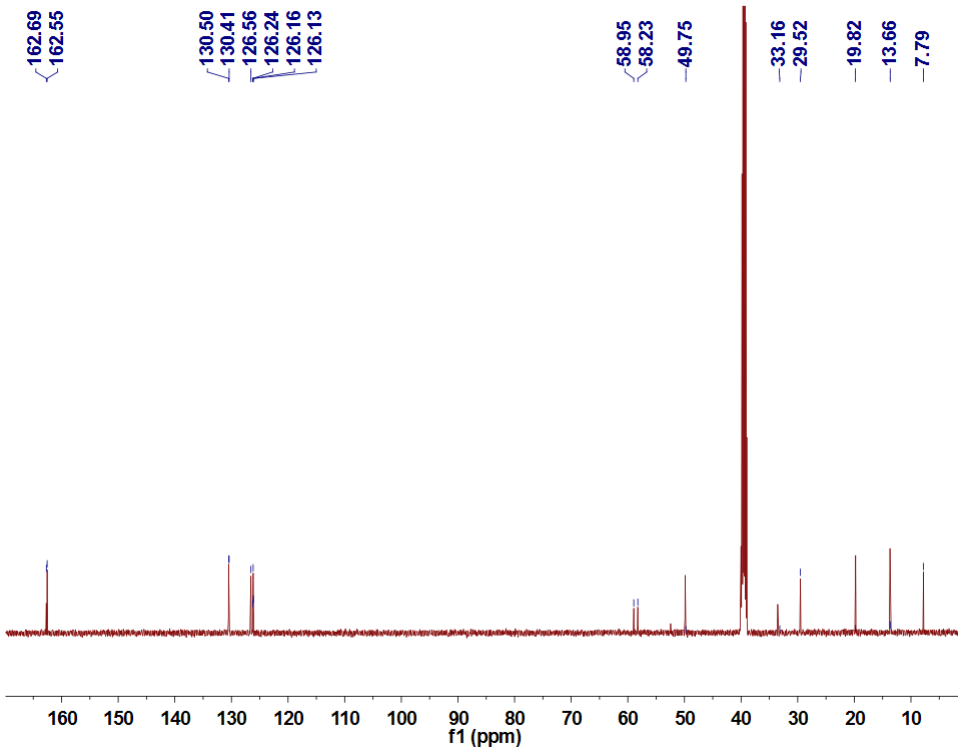

Fig. S11 ^{13}C NMR spectrum (125 MHz, DMSO-d_6, room temperature) of **M**.

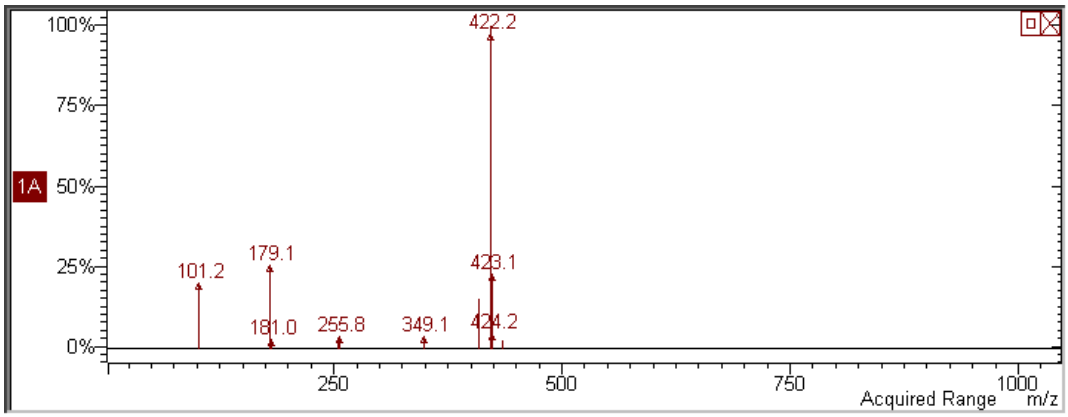

Fig. S12 Electrospray ionization mass spectrum of **M**. Assignment of main peaks: *m/z* 422.2 $[M - Br]^+$.

*4. 2D COSY spectrum of **M** in D_2O*

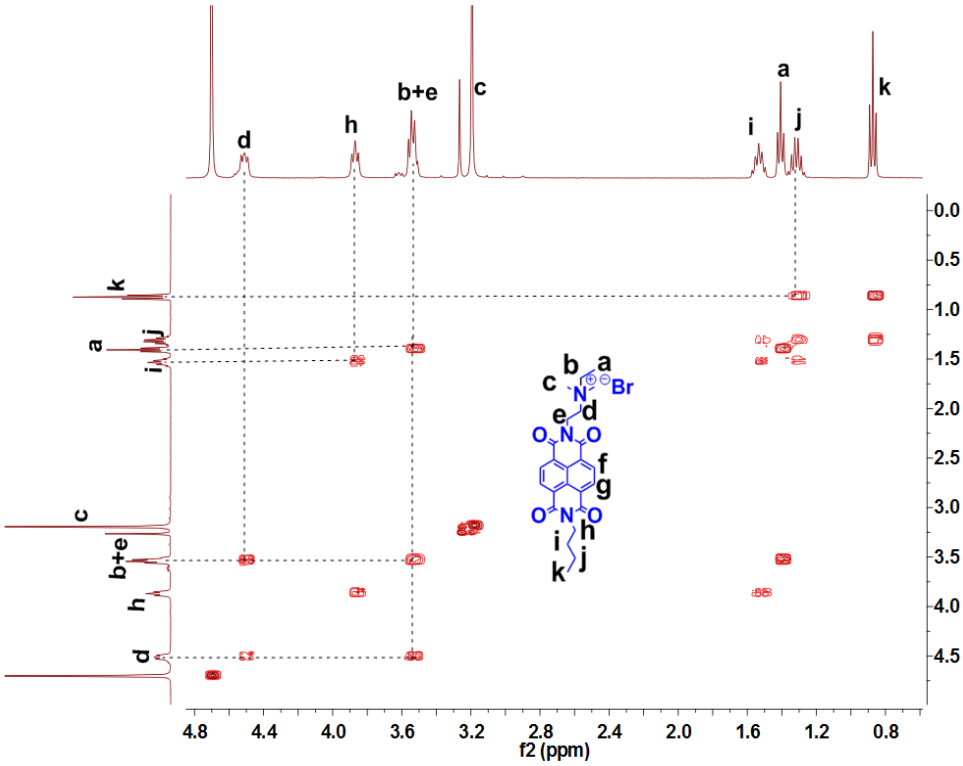

Fig. S13 2D ^{1}H-^{1}H COSY spectrum (400 MHz, D_2O, 298 K) of **M**.

*5. The sizes of pillar[5]arenes, pillar[6]arenes, pillar[7]arenes and **G***

From previous work,[S2] the diameters of the internal cavities of pillar[5]arenes, pillar[6]arenes and pillar[7]arenes were calculated to be ~4.7, ~6.7 and ~8.7 Å, respectively, by treating pillar[5]arenes, pillar[6]arenes and pillar[7]arenes as regular pillars and ignoring the influence of the substituents on the oxygen atoms (Scheme

S3). On the other hand, the size of **G** in its energy-minimized structure was calculated by using Chem 3D (Scheme S4).

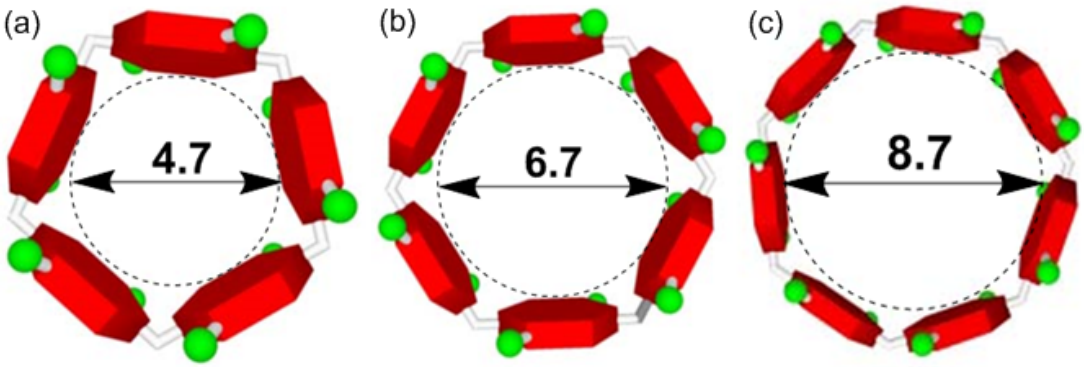

Scheme S3. The cavity sizes of pillar[5]arenes (a), pillar[6]arenes (b) and pillar[7]arenes (c). We used the van der Waals radii of the atoms to calculate the sizes.

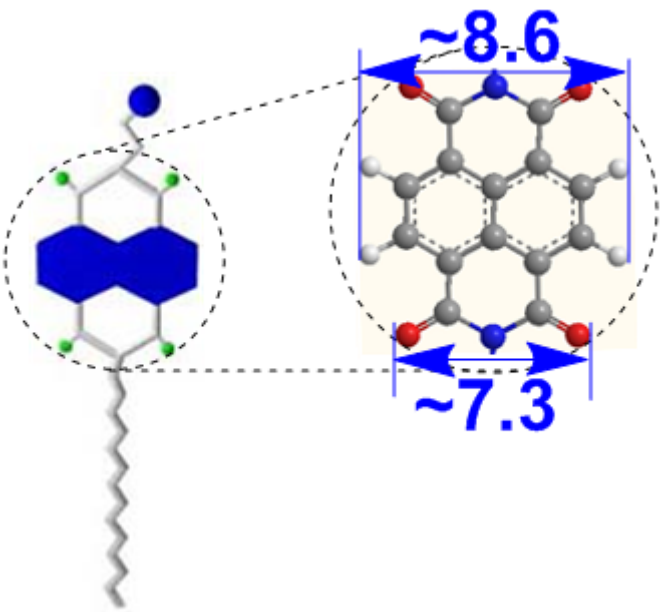

Scheme S4. The size (Å) of the NDI group. We used the van der Waals radii of the atoms to calculate the size.

*6. ^{1}H NMR spectroscopic investigations of **WP7⊃M**, **WP6⊃M** and **WP5⊃M***

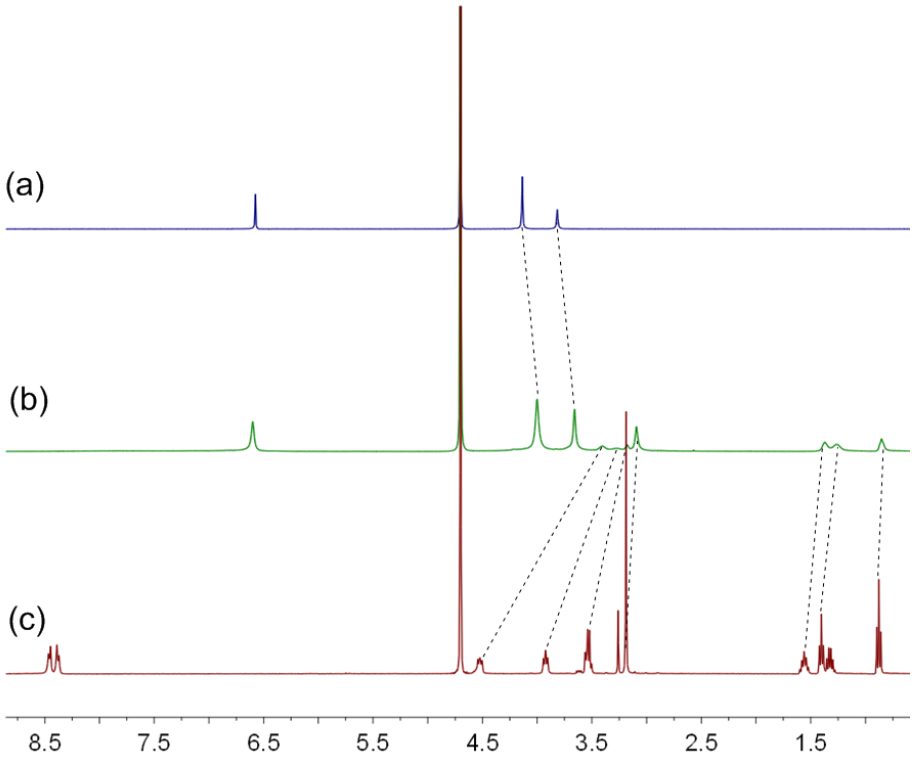

Fig. S14 Partial ^{1}H NMR spectra (400 MHz, D_2O, room temperature): (a) **WP7** (2.00 mM); (b) **M** (2.00 mM) and **WP7** (2.00 mM); (c) **M** (2.00 mM).

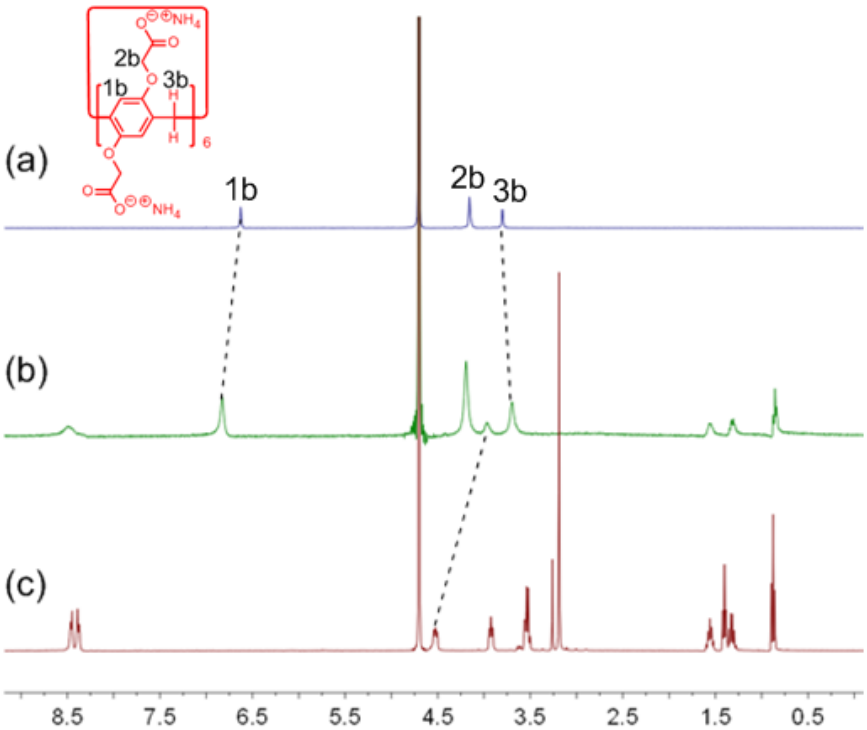

Fig. S15 Partial ^{1}H NMR spectra (400 MHz, D_2O, room temperature): (a) **WP6** (2.00 mM); (b) **M** (2.00 mM) and **WP6** (2.00 mM); (c) **M** (2.00 mM).

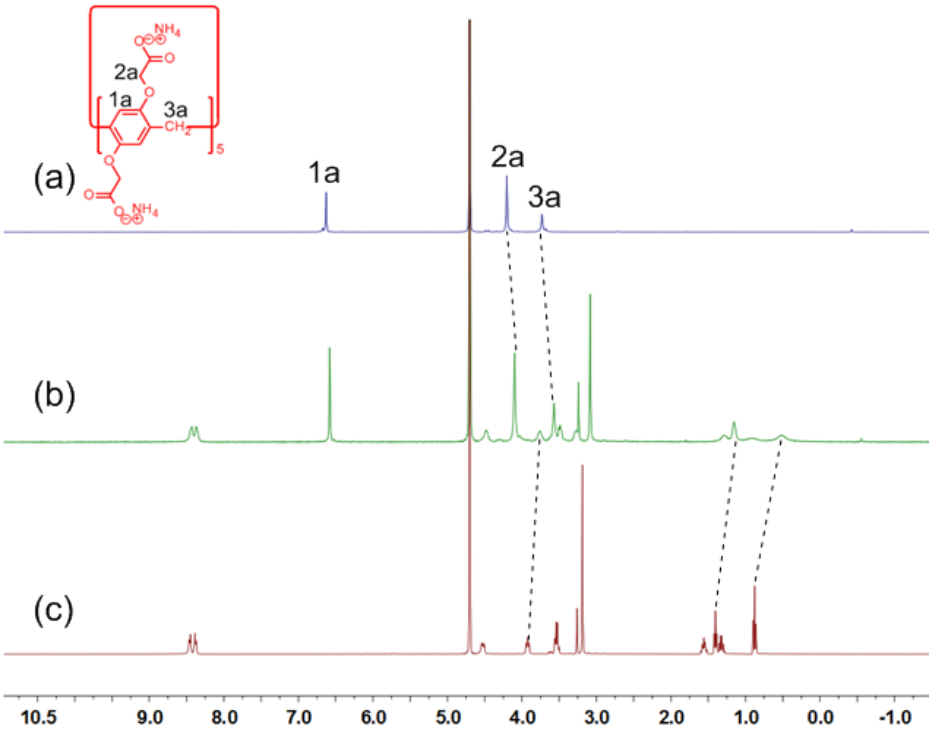

Fig. S16 Partial ^{1}H NMR spectra (400 MHz, D_2O, room temperature): (a) **WP5** (2.00 mM); (b) **M** (2.00 mM) and **WP5** (2.00 mM); (c) **M** (2.00 mM).

*7. Critical aggregation concentration (CAC) determinations of **G** and **WP7⊃G***

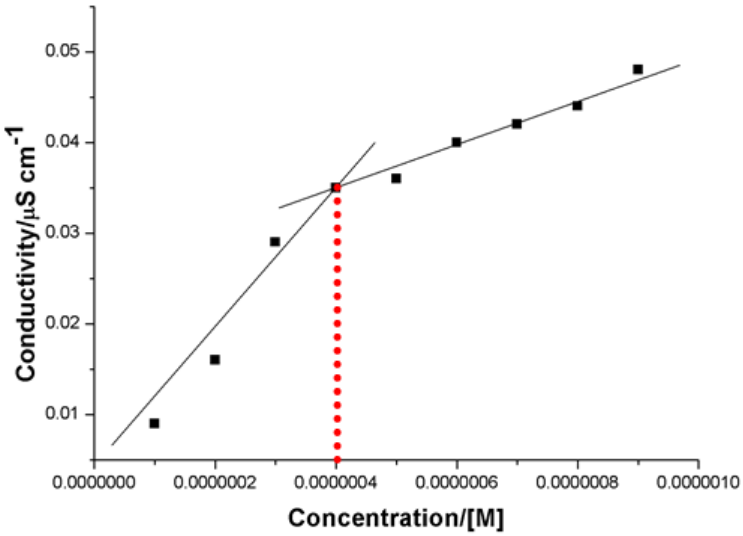

Fig. S17 The concentration-dependent conductivity of **G**. The critical aggregation concentration (CAC) was determined to be 4.02×10^{-7} M.

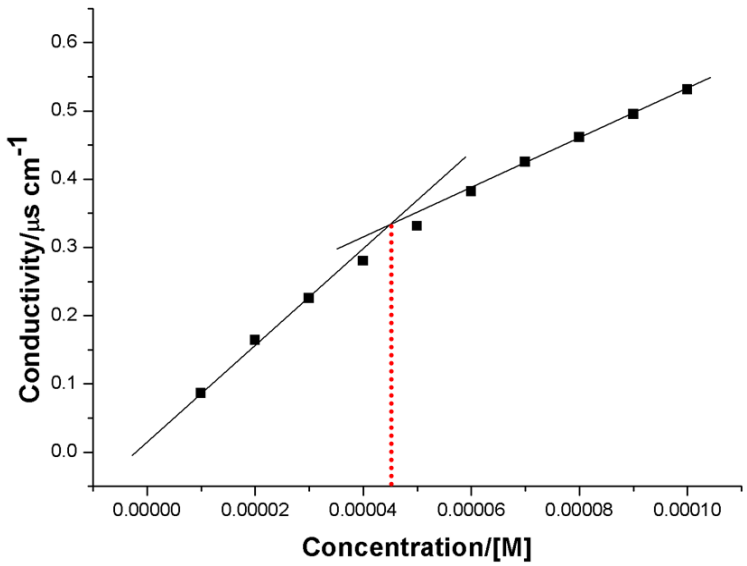

Fig. S18 The concentration-dependent conductivity of equimolar **WP7** and **G**. The critical aggregation concentration (CAC) was determined to be 4.49×10^{-5} M.

*8. Dynamic light scattering (DLS) results of **WP7⊃G** in the absence and presence of 1 equiv. α-CD*

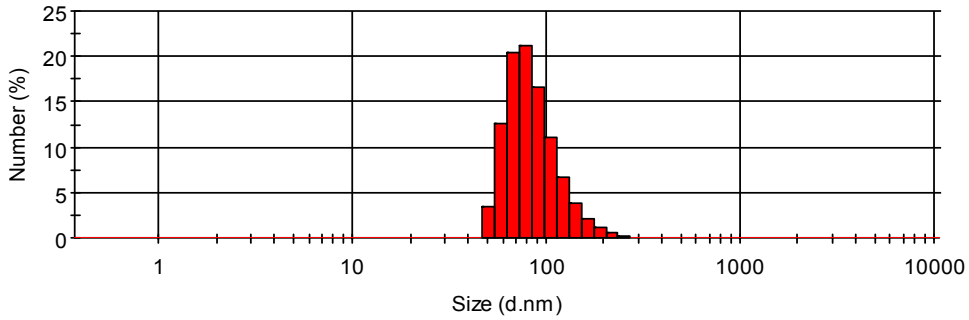

Fig. S19 DLS result of **WP7** (3.57×10^{-5} M) and **G** (5.00×10^{-5} M). The average diameter of the nanospheres was determined to be 87 nm.

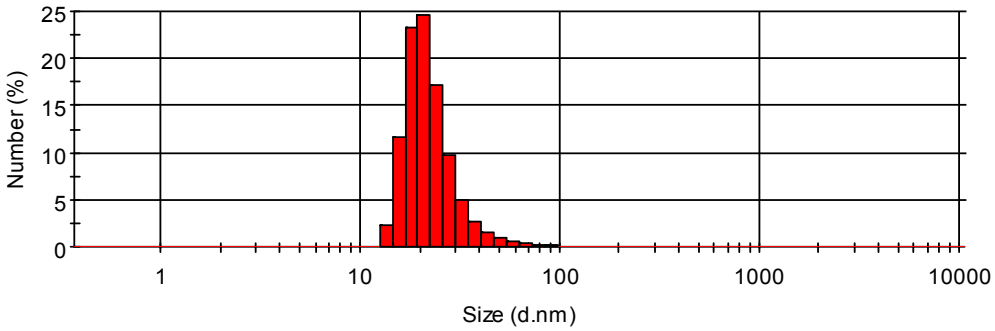

Fig. S20 DLS result of **WP7** (3.57×10^{-5} M) and **G** (5.00×10^{-5} M) in the presence of 1 equiv. α-CD. The average diameter of the nanospheres was determined to be 23 nm.The

diameter of the nanoparticles determined by DLS was larger than that determined by TEM, because the nanoparticles might aggregated together to form larger aggregates in solution state.

*9. The ^{1}H NMR of **WP7⊃M** with different molar ratios*

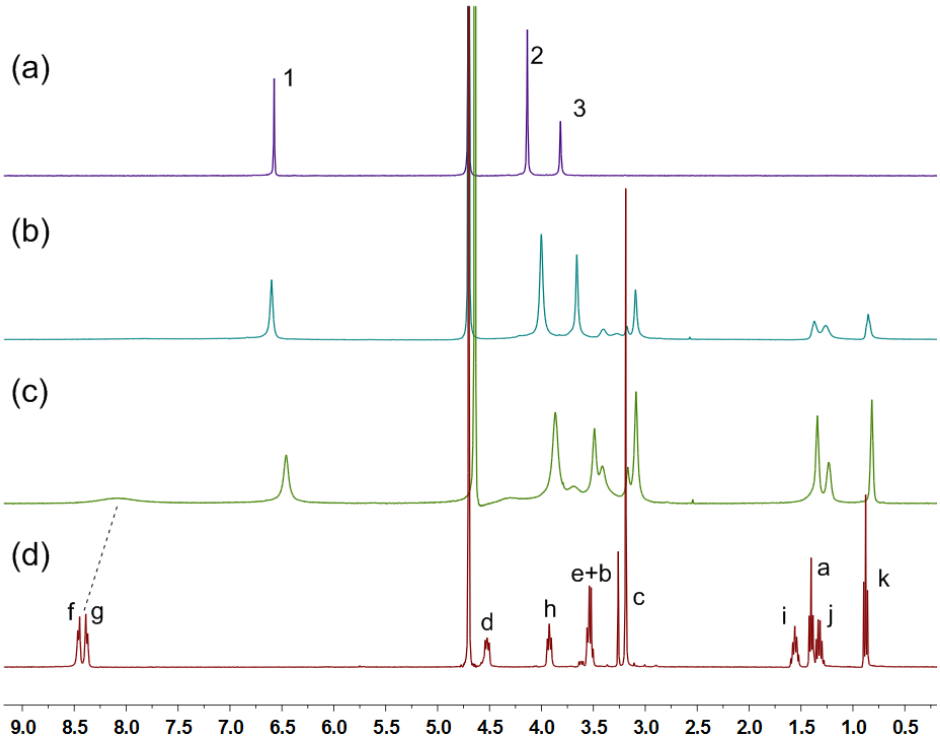

Fig. S21 Partial ^{1}H NMR spectra (400 MHz, D_2O, room temperature): (a) **WP7** (2.00 mM); (b) **WP7** (2.00 mM) and **M** (2.00 mM); (c) **WP7** (2.00 mM) and **M** (6.00 mM); (d) **M** (2.00 mM).

*10. Enlarged TEM images of **WP7⊃G** in the presence of 1 equiv. α-CD.*

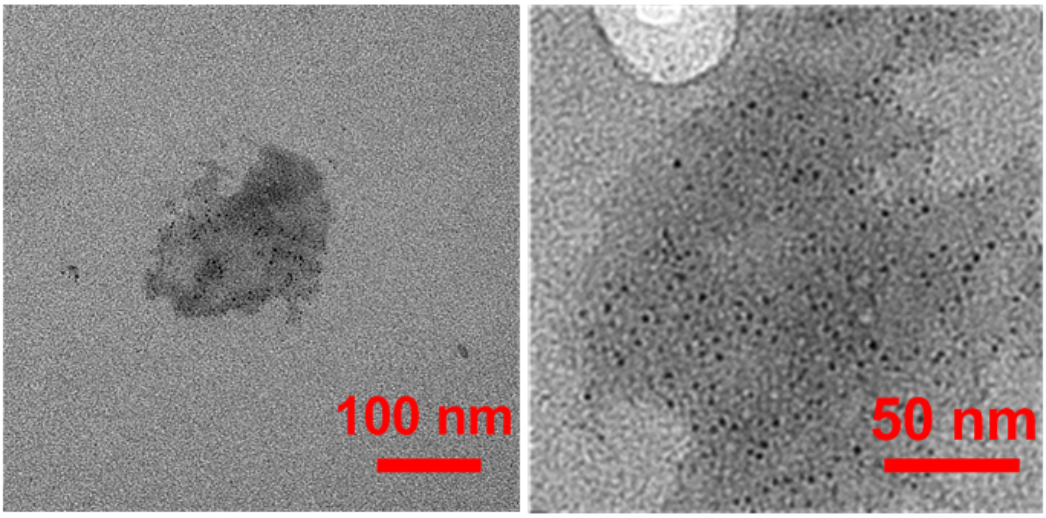

Fig. S22 Enlarged TEM images of **WP7⊃G** in the presence of 1 equiv. *α*-CD.

*11. ITC investigations of host−guest complexation between **WP7** and **M**, **WP6** and **M**, **WP5** and **M**, **M** and α-CD, **WP7**⊃**M** and α-CD.*

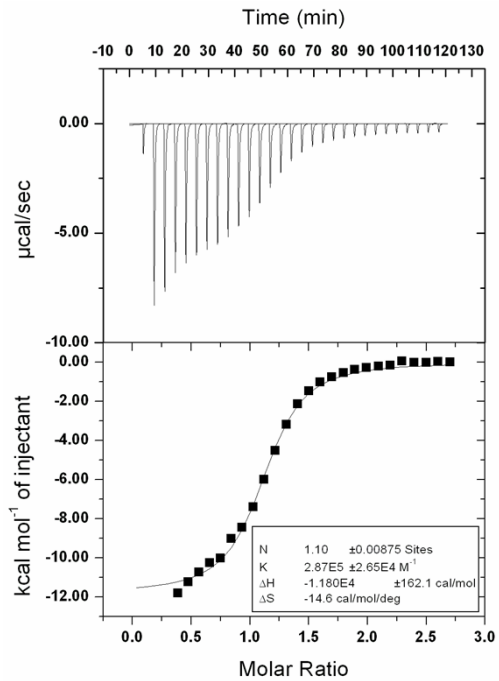

Figure S23. Microcalorimetric titration of **WP7** (2.00 mM, 10 μL per injection) with **M** (0.100 mM) in water at 298.15 K. Top: raw ITC data for 29 sequential injections (10 μL per injection) of a **WP7** solution (2.00 mM) into an **M** solution (0.100 mM); bottom: net reaction heat obtained from the integration of the calorimetric traces.

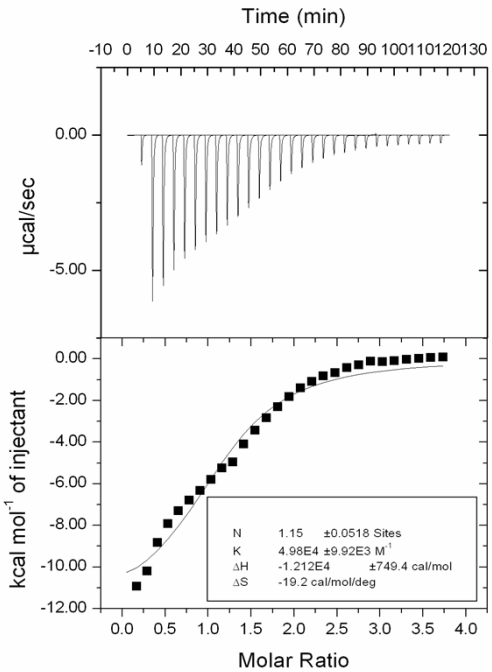

Figure S24. Microcalorimetric titration of **WP6** (2.00 mM, 10 μL per injection) with **M** (0.100 mM) in water at 298.15 K. Top: raw ITC data for 29 sequential injections (10 μL per injection) of a **WP6** solution (2.00 mM) into an **M** solution (0.100 mM); bottom: net reaction heat obtained from the integration of the calorimetric traces.

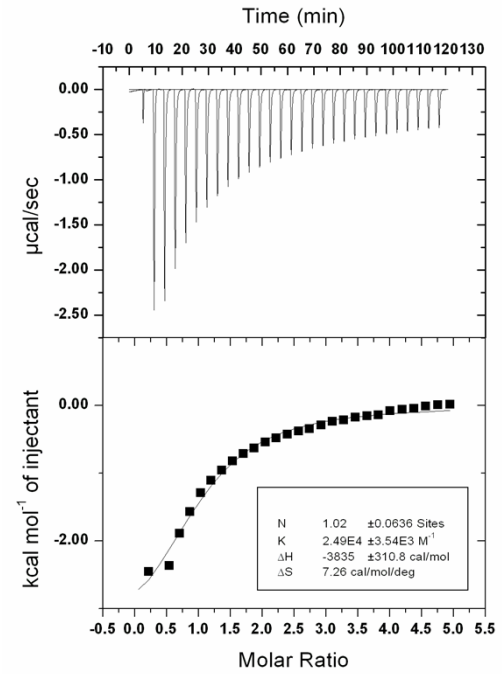

Figure S25. Microcalorimetric titration of **WP5** (2.00 mM, 10 µL per injection) with **M** (0.100 mM) in water at 298.15 K. Top: raw ITC data for 29 sequential injections (10 µL per injection) of a **WP5** solution (2.00 mM) into an **M** solution (0.100 mM); bottom: net reaction heat obtained from the integration of the calorimetric traces.

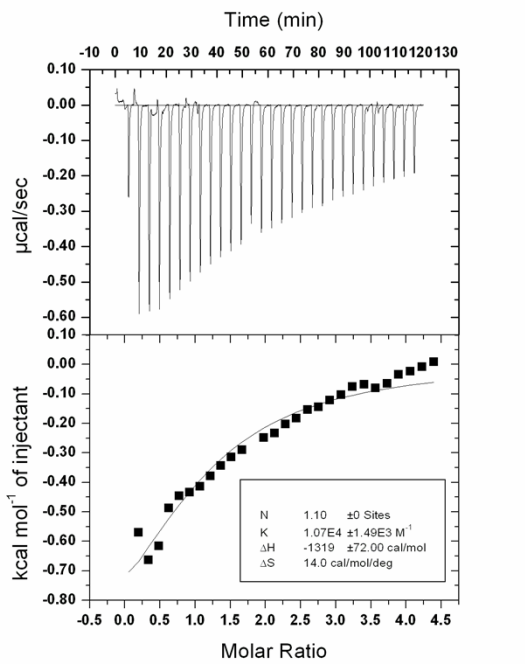

Figure S26. Microcalorimetric titration of α-CD (2.00 mM, 10 µL per injection) with **M** (0.100 mM) in water at 298.15 K. Top: raw ITC data for 29 sequential injections (10 µL per injection) of an α-CD solution (2.00 mM) into an **M** solution (0.100 mM); bottom: net reaction heat obtained from the integration of the calorimetric traces.

*12. Fluorescence spectroscopy studies of **M** and **WP7⊃M** after the addition of α-CD*

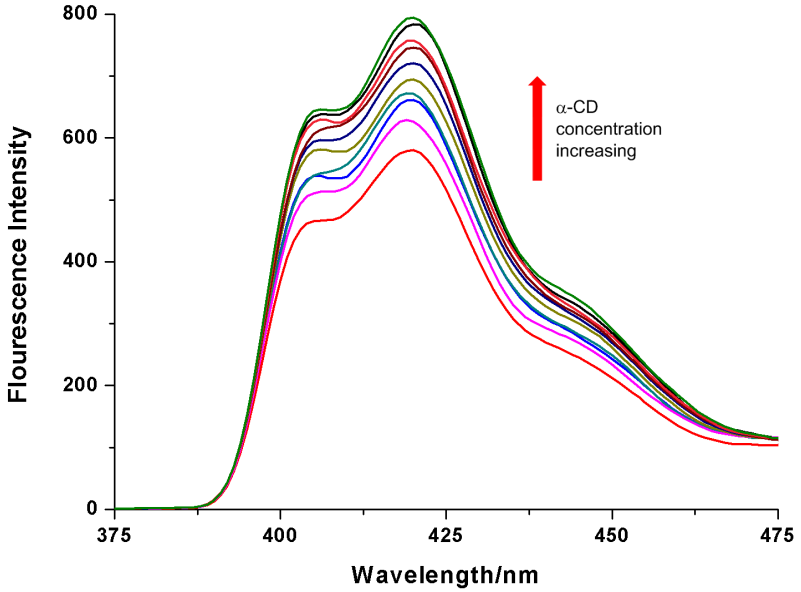

Figure S27. Fluorescence spectra of **M** (2.00 × 10^{-4} M) in aqueous solution at room temperature with different concentrations of *α*-CD: 0, 0.080, 0.100, 0.200, 1.00, 2.00, 3.00, 4.00, 5.00 and 6.00× 10^{-4} M.

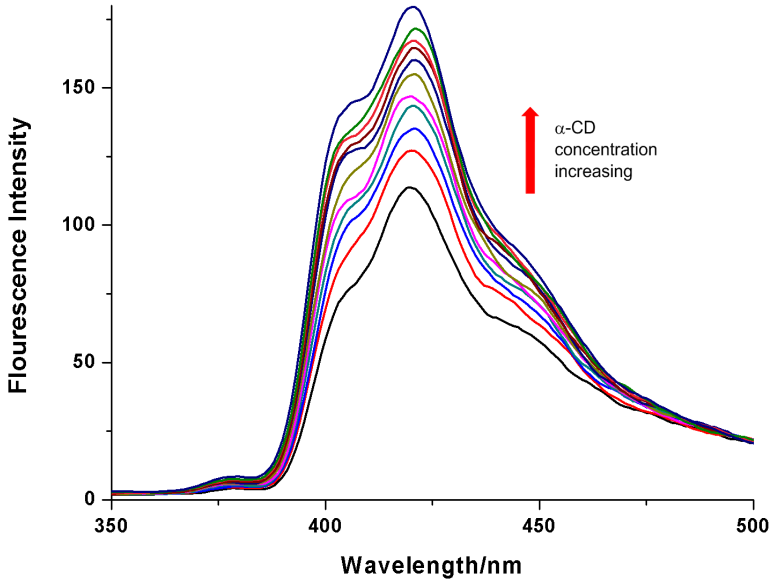

Figure S28. Fluorescence spectra of **WP7⊃M** (5.00 × 10^{-5} M) in aqueous solution at room temperature with different concentrations of *α*-CD: 0, 1.00, 2.00, 3.00, 4.00, 5.00, 6.00, 7.00 8.00, 9.00 and 10.00 × 10^{-4} M.

*13. 2D NOESY NMR spectrum of **M** and α-CD in D_2O*

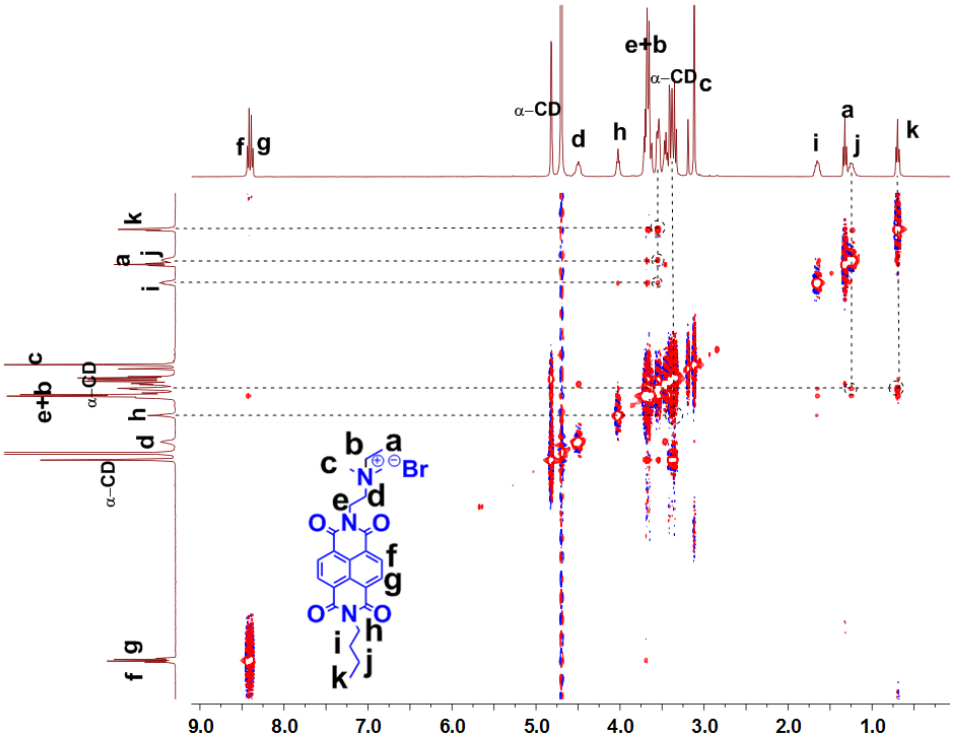

Figure S29. Partial NOESY NMR spectrum (400 MHz, D_2O, room temperature) of **M** (10.0 mM) and *α*-CD (10.0 mM).

***References**:*

S1. Z. Li, J. Yang, G. Yu, J. He, Z. Abliz and F. Huang, *Org. Lett.*, 2014, **16**, 2066−2069.

S2. C. Han, Z. Zhang, X. Chi, M. Zhang, G. Yu and F. Huang, *Acta Chim. Sinica*, 2012, **70,** 1775−1778.